Halide substitution in Ca(BH4)2

Halide substitution in $Ca(BH_4)_2$

Hilde Grove[1], Line H. Rude[2], Torben R. Jensen[2], Marta Corno[3], Piero Ugliengo[3], Marcello Baricco[3], Magnus H. Sørby[1], Bjørn C. Hauback[1]

[1] *Institute for Energy Technology, P.O. Box 40 Kjeller, NO-2027, Norway*

[2] *Center for Materials Crystallography (CMC), Interdisciplinary Nanoscience Center (iNANO), and Department of Chemistry, Aarhus University, Langelandsgade 140, DK-8000 Århus C, Denmark.*

[3] *Dipartimento di Chimica and NIS, Università di Torino, Via P.Giuria 7, I-10125 Torino, Italy.*

Abstract

Halide substitution in $Ca(BH_4)_2$ has been investigated in ball milled mixtures of $Ca(BH_4)_2$ and CaX_2 (X = F, Cl, Br) with different molar ratios. In-situ synchrotron radiation powder X-ray diffraction measurements of $Ca(BH_4)_2$ + $CaCl_2$ with 1:0.5, 1:1 and 1:2 molar ratios reveal that no substitution of Cl^- for BH_4^- occurs from the ball milling process. However, substitution readily occurs after the transition from α- to β-$Ca(BH_4)_2$ upon heating above ~250 °C, which is evident from both contraction of the unit cell and changes in the relative Bragg peak intensities, in agreement with theoretical calculations. Rietveld analyses of the obtained β-$Ca((BH_4)_{1-x}Cl_x)_2$ solid solutions indicate compositions from x = 0 to 0.6, depending on the amount of $CaCl_2$ in the parent mixtures. β-$Ca((BH_4)_{0.5}Cl_{0.5})_2$ was investigated by differential scanning calorimetry and has a slightly higher decomposition temperature compared to pure $Ca(BH_4)_2$. No substitution with CaF_2 or $CaBr_2$ is observed.

1. Introduction

The efforts to find fuels that are non-polluting and not contributing to the greenhouse effect is on-going. Hydrogen is a clean energy carrier, releasing only water when used in fuel cells. Hydrogen is a gas with low boiling point and consequently the challenge for hydrogen to become a widely used energy carrier is an efficient storage system. It is possible to store hydrogen gas under pressure, but a safer and much more compact way is to store hydrogen chemically bonded in solid compounds.[1] The storage material should

have both high gravimetric and volumetric hydrogen content, good cycling ability and fast hydrogen sorption kinetics. $NaAlH_4$ with titanium-based additives was the first complex metal hydrides to be considered for hydrogen storage[2], but the practical gravimetric hydrogen storage capacity is less than 4.5 wt%.[3] Metal borohydrides have high gravimetric hydrogen density and are thus of interest as hydrogen storage materials.[4,5] $Ca(BH_4)_2$ can theoretically store up to 11.6 wt% hydrogen and the volumetric hydrogen content is 108 g H/L. DFT calculation estimates an equilibrium H_2 pressure of 1 bar at temperatures below 100 °C,[6] which is ideal for hydrogen storage for mobile applications. Experimentally, however, the dehydrogenation process occurs between 360 and 500 °C.[6-8] The hydrogen sorption is partially reversible at 90 bar and temperatures from 350 to 420 °C.[7] $Ca(BH_4)_2$ is generally observed to decompose to CaB_6 and CaH_2, according to the reaction $3Ca(BH_4)_2 \rightarrow CaB_6 + 2CaH_2 + 10H_2$, but the process is complicated and several intermediate phases are involved.[9-12]

The observed dehydrogenation temperature is too high for practical purposes,[1] thus the stability has to be reduced for $Ca(BH_4)_2$ to become an effective energy carrier. Brinks *et. al.* have shown that the stability of Na_3AlH_6 can be considerably changed by partly substituting hydrogen with fluorine.[13] Several studies have shown that that heavier halides can substitute BH_4^- in borohydrides, e.g. Cl^-, Br^-, and I^- substitution in $LiBH_4$,[14-18] and Cl^- substitution in $NaBH_4$[18] and $Mg(BH_4)_2$[19]. Recently, three new compounds have been reported in the $Ca(BH_4)_2$–CaI_2 system.[20]

Several structural modifications of $Ca(BH_4)_2$ have been described in the literature.[6,21-27] α-$Ca(BH_4)_2$ (orthorhombic, space group *F*2*dd*) is the stable polymorph at room temperature.[22,28] It transforms to tetragonal α'-$Ca(BH_4)_2$ through a second-order transformation around 220°C and further completely to β-$Ca(BH_4)_2$ upon heating above 300°C.[22] The β-phase crystallizes with tetragonal symmetry first described in space group $P4_2/m$[23] and later revised to $P\bar{4}$[22,26,29,30]. γ-$Ca(BH_4)_2$ is sometimes formed at room temperature. This phase is metastable and crystallizes in the orthorhombic space group *Pbca*.[10,28]

The purpose of this work is to study possible substitution of F^-, Cl^- and Br^- in $Ca(BH_4)_2$. The most likely substitute for hydrogen is fluorine, because of the similarity in size. On

the other hand, the BH_4^--ion has similar size (2.05 Å) to both the Cl^--ion (1.81 Å) and the Br^- ion (1.96 Å). These halides might therefore substitute the whole BH_4^- group.

2. Experimental and theoretical methods

2.1 Preparation of $Ca(BH_4)_2$ + CaX_2 samples

$Ca(BH_4)_2 \cdot 2THF$ (purchased from Sigma Aldrich) was dried in vacuum ($p \approx 1 \cdot 10^{-1}$ mbar) at 160 °C for 24 hours to remove the THF adducts, which yielded a mixture of the α and β polymorphs of $Ca(BH_4)_2$ after cooling to ambient temperature. The calcium halides, CaX_2, X = F, Br (Aldrich, purity: 99.99%, 99.98%, respectively) and X = Cl (Alfa Aesar, purity: 99.9%) were used as purchased.

The solvent-free $Ca(BH_4)_2$ was mixed with CaX_2 in molar ratios of 1:0.5 (X = F, Cl) , 1:1 (X = Cl, Br) or 1:2 (X = Cl) and ball milled for 2 hours (2 min milling, 2 min pause, times 60) under argon atmosphere with a ball-to-powder ratio of approximately 30:1 using tungsten carbide bowl (15 mL) and balls (10 mm) in a Fritsch Pulverisette P4. The bowl was sealed with a lid and a polymer O-ring.

All handling of the materials was done in purified Ar atmosphere (< 1 ppm O_2 and H_2O) in an MBraun glove box.

2.2 In situ Synchrotron Radiation Powder X-ray Diffraction

In situ synchrotron radiation powder X-ray diffraction (SR-PXD) was performed at beamline BM01A at the Swiss-Norwegian Beamlines (SNBL) at European Synchrotron Radiation Facility (ESRF) in Grenoble, France. A MAR345 image plate detector was used and the samples were packed in boronglass capillaries (0.5 mm) and connected to a vacuum pump. The X-ray exposure time for each measurement was 30 s and the readout time was 90 seconds, thus a complete SR-PXD diagram was collected every second minute. The wavelengths used were λ = 0.703511 Å or 0.654780 Å. The wavelength and detector geometry were calibrated with LaB_6 as an external standard. Different heating rates were used, 3 K/min was used for all $Ca(BH_4)_2$ + $CaCl_2$ samples, 2 and 3 K/min were used for other samples.

One-dimensional diffraction patterns were obtained by integrating the 2D images using the Fit2D program. [31] Data analyses were performed using the Rietveld method in the

FullProf suite. [32] The background was interpolated between manually selected points and the Bragg peaks where modeled by a pseudo-Voigt function with 3 refinable parameters.

2.3 Thermal Analysis

Differential scanning calorimetry (DSC) was performed with a Netzsch STA449C Jupiter instrument at heating rates of 10 K/min in a flow of He (50 mL/min). The samples were contained in Al_2O_3 crucibles with tiny holes in the lid to prevent pressure build-up during desorption of gases.

2.4 Computational Details

The calculations were performed applying the periodic quantum-mechanical software CRYSTAL09 within the Density Functional Theory, PBE functional. The CRYSTAL code utilizes localized Gaussian functions to describe electrons. Ca was described by a 86-511d21G all-electron basis set[33]; B by a 6-21G(d) basis set (α_{sp} = 0.124 bohr^{-2} for the most diffuse shell exponent and α_{pol} = 0.800 bohr^{-2} for polarization); H by a 31G(p) (α_{sp} = 0.1613 bohr^{-2} for the most diffuse shell exponent and α_{pol} = 1.1 bohr^{-2} for polarization),[34] F by a 7-311G(d),[35] Cl by a 86-311G with an additional d orbital (α_{sp} = 0.125 bohr^{-2} for the most diffuse shell exponent and α_d = 0.750 bohr^{-2}) [36] and Br by a 6-311G(d) (α_d = 0.154 bohr^{-2} for the most diffuse shell exponent and α_{pol} =0.451 bohr^{-2} for polarization).[37] Grimme correction was also considered to take the dispersive contributions into account in all the calculations for geometry optimization and energetic description.[38] Phonons at Γ point in the harmonic approximation were computed to derive the thermodynamic functions by diagonalizing the associated mass-weighted Hessian matrix.[39]

3. Results and Discussion

3.1 The $Ca(BH_4)_2$–CaF_2 system

For $Ca(BH_4)_2$–CaF_2 with molar ratio 1:0.5, the four phases α-, β-, and γ-$Ca(BH_4)_2$ and CaF_2 are observed in the diffraction pattern of the as-milled sample. The amount of CaF_2, compared to the amount of $Ca(BH_4)_2$ calculated from the SR-PXD data, indicates that no F-substitution had occurred. During heating, the phase transformation from the α- to the β-modification is observed between 160 and 220 ^{o}C, in addition to the changes in unit

cell parameters due to the thermal expansion. The intensities corresponding to the Bragg peaks from CaF_2 do not decrease and there were no significant changes in the relative intensities of the Bragg peaks from $Ca(BH_4)_2$. This indicates that there is no fluorine substitution neither in the α nor in the β polymorph of $Ca(BH_4)_2$.

3.2 The $Ca(BH_4)_2$–$CaCl_2$ system

After ball milling $Ca(BH_4)_2$ and $CaCl_2$ in the molar ratios 1:0.5, 1:1 and 1:2, α-$Ca(BH_4)_2$ is the most prominent $Ca(BH_4)_2$ polymorph, but a residue of the β-phase is also observed by SR-PXD. $CaCl_2$ is observed in its stable modification (space group *Pnnm*), but it is also present in two other modifications with space groups *Pbcn* [40] and *Pbca* [41] in the milled $Ca(BH_4)_2$–$CaCl_2$ samples. The latter is a high pressure $CaCl_2$ polymorph formed from the *Pbcn* phase during milling. Some additional peaks from minor impurity phases are also observed, but they have been disregarded in the Rietveld refinements.

The sample $Ca(BH_4)_2$–$CaCl_2$ 1:1 was studied with SR-PXD during heating up to 360 °C, and the results are shown in Figure 1. Rietveld refinement of the SR-PXD data collected at about 40 °C gives α-$Ca(BH_4)_2$ (36 wt%), $CaCl_2$ *Pnnm* (20 wt%) and $CaCl_2$ *Pbca* (33 wt%) as the main components, with minor amounts of β-$Ca(BH_4)_2$ (2 wt%) and $CaCl_2$ *Pbcn* (7 wt%). $Ca(BH_4)_2$ and $CaCl_2$ in 1:1 molar ratio corresponds to a mass ratio of 39:61. This is close to the refined values when summing all the $Ca(BH_4)_2$ phases and $CaCl_2$ phases: 38 wt% and 62 wt%, respectively. This indicates that most of the sample is crystalline and also that no reaction between the compounds has occurred during ball milling. The refined unit cell parameters for α-$Ca(BH_4)_2$ at 40 °C are: a = 8.755(6) Å, b = 13.143(6) Å and c = 7.532(5) Å. These are in good agreement with literature values (see Table 1) and the relative intensities of the Bragg peaks from α-$Ca(BH_4)_2$ fits well with published crystal structure data [26], thus supporting that no substitution has taken place at this temperature. Substitution would be evident as a decrease in the unit cell size and marked changes in the relative intensities due to the smaller size and higher X-ray scattering cross section for Cl^- compared to BH_4^-.

Table 1 Crystallographic parameters for pure and chloride containing $Ca(BH_4)_2$ compounds at different temperatures

Compound	Crystal System	Space group	*a*/Å	*b*/Å	*c*/Å	V/Å^3	T/°C
α-$Ca(BH_4)_2$ [26]	Orthorhombic	*F*2*dd*	8.745	13.105	7.495	858.95	RT
α-$Ca(BH_4)_2$ *	Orthorhombic	*F*2*dd*	8.755(6)	13.143(6)	7.532(5)	867(1)	40
β-$Ca(BH_4)_2$[22]	Tetragonal	*P*-4	6.9189(1)		4.3471(1)	208.1	RT
β-$Ca(BH_4)_2$ [29]	Tetragonal	*P*-4	6.9509(5)		4.3688(3)	211.1(2)	160
β-$Ca(BH_4)_2$ [42]	Tetragonal	*P*-4	7.005(5)		4.414(7)	216.6(4)	350
β-$Ca((BH_4)_{0.7}Cl_{0.3})_2$ *	Tetragonal	*P*-4	6.7725(6)		4.3074(6)	197.6(1)	350
β-$Ca((BH_4)_{0.5}Cl_{0.5})_2$ *	Tetragonal	*P*-4	6.673(4)		4.268(2)	190.0(2)	350
β-$Ca((BH_4)_{0.4}Cl_{0.6})_2$ *	Tetragonal	*P*-4	6.542(3)		4.214(2)	180.3(1)	350

**This work*

The phase transformation from α-$Ca(BH_4)_2$ to β-$Ca(BH_4)_2$ takes place in the temperature range 150-200 °C, see Figure 1. At about 260 °C a shoulder starts to appear on the high angle side of the β-$Ca(BH_4)_2$ peaks. Upon further heating, the diffraction peaks from the β-polymorph is gradually shifted to higher scattering angle, indicating contraction of the unit cell. This is in agreement with substitution of BH_4^- with the smaller Cl^-. The following reaction seems to take place:

$$\beta\text{-}Ca(BH_4)_2 + x\ CaCl_2 \rightarrow (1+x)\ \beta\text{-}Ca((BH_4)_{1-x}Cl_x)_2$$

Furthermore, from the Rietveld refinement the relative intensities of the peaks for the proposed β-$Ca((BH_4)_{1-x}Cl_x)_2$ do not match the diffraction pattern for pure β-$Ca(BH_4)_2$. Exchanging some of the BH_4^- with Cl^- in the Rietveld refinement of β-$Ca(BH_4)_2$, results in a better fit to the observed data. Figure 2 shows the refinement for substituted $Ca((BH_4)_{1-x}Cl_x)_2$ giving x = 0.53(3) at 350 °C.

The onset of chloride substitution in β-$Ca(BH_4)_2$ follows shortly after the reported phase transformation temperature of $CaCl_2$ from the orthorhombic *Pnnm* phase to a tetragonal phase described in space group $P4_2/mnm$ at 235 °C. [43] The transition is of the second-order and proceeds by contraction of the *a*-axis and expansion of the *b*-axis in the orthorhombic phase until they become identical at the phase transition temperature. It is interesting to note that this high-temperature phase of $CaCl_2$ (HT-$CaCl_2$) can be regarded as isostructural to β-$Ca(BH_4)_2$ if the non-spherical symmetry of BH_4^- is disregarded. The difference in space group, $P4_2/mnm$ vs *P*-4, is due to the tetrahedral symmetry of the BH_4^- anion compared to spherical symmetry of Cl^-. The phase transformation of $CaCl_2$ induce only subtle changes in the diffraction pattern which are not directly observable in the

present data, due to extensive peak overlap with $Ca(BH_4)_2$. However, HT-$CaCl_2$ was used in Rietveld refinements of data collected above the transition temperature, resulting in good fits to the data.

For the sample with molar ratio 1:1, the refinements show that there is still 15 wt% of $CaCl_2$ left in the sample at 350 °C, suggesting that the substituted fraction x in $Ca(BH_4)_2$ must be somewhat smaller than 0.5. Specifically, calculation of the degree of substitution from the weight fractions of the different phases gives x = 0.45(5). For the 1:2 and 1:0.5 samples at 350 °C, the Rietveld refinements of anion site occupancies give compositions x = 0.81(1) and x = 0.46(2), respectively. From the refined phase fractions x should be 0.60(6) for the 1:2 sample and 0.30(3) for the 1:0.5 sample. Thus, the refined ratios of the BH_4^- and Cl^- in the three substituted phases all overestimate the amounts of Cl^- compared to the nominal compositions. This could be due to the high anisotropy of BH_4^-, making it difficult to determine exact positions of the H atoms and, consequently, making refinement less stable. The compositions estimated from the phase fractions, i.e. from the ratio of unreacted $CaCl_2$ and substituted $Ca(BH_4)_2$, are deemed to be more reliable. Hence, the compositions of the three substituted phases are given with one decimal precision as $Ca((BH_4)_{0.5}Cl_{0.5})_2$ (x=0.5), $Ca((BH_4)_{0.4}Cl_{0.6})_2$ (x = 0.6) and $Ca((BH_4)_{0.7}Cl_{0.3})_2$ (x = 0.3) for the samples 1:1, 1:2 and 1:0.5, respectively.

Table 1 shows significant contraction in unit cell dimensions for all Cl-substituted β-$Ca(BH_4)_2$ sample. The changes are anisotropic with larger changes in the a-axis than the c-axis. This is can be explained by a greater difference in the a-axis than the c-axis between pure β-$Ca(BH_4)_2$ (a = 7.0 Å, c = 4.4 Å at 350ºC) and HT-$CaCl_2$ (a = 6.4 Å, c = 4.2 Å at 350ºC) [43]. The changes in unit cell parameters are approximately proportional to the amount of Cl substitution into the lattice, in agreement with Vegard's law.[44]

DSC measurements were performed for pure $Ca(BH_4)_2$ and $Ca(BH_4)_2$–$CaCl_2$ ball milled in molar ratio 1:1, respectively, see Figure 3. For the pure $Ca(BH_4)_2$, there is a sharp endothermic peak in the DSC data at about 370°C. This is consistent with release of hydrogen from $Ca(BH_4)_2$. The same feature is seen in the 1:1 $Ca(BH_4)_2$–$CaCl_2$ sample, but the temperature of the event is increased to 390°C, indicating a slight stabilization of the Cl-containing compound. SR-PXD data show that CaHCl is a decomposition product.

This is in agreement with our recent report that the $Ca(BH_4)_2$ - CaI_2 decompose to CaHI [20]. No other crystalline decomposition products are observed in the present study.

3.3. The $Ca(BH_4)_2$ – $CaBr_2$ system

$Ca(BH_4)_2$ and $CaBr_2$ were ball milled in the molar ratio 1:1. $CaBr_2$ (V = 196 $Å^3$) is isostructural with the *Pnnm* modification of $CaCl_2$ (168 $Å^3$). When the $Ca(BH_4)_2$ – $CaBr_2$ sample is heated, the SR-PXD data shows the transformation from α- to β-$Ca(BH_4)_2$ in the temperature range 150-200 °C. There are no significant changes in unit cell parameters beside thermal expansion, no change in relative intensities of the β-$Ca(BH_4)_2$ diffraction peaks and the intensities of the $CaBr_2$ peaks do not decrease. This indicates that no appreciable amount of Br^- is substituted into $Ca(BH_4)_2$, which is confirmed with Rietveld refinement showing a good fit without any substitution. The lack of substitution can be explained by the high transition temperature of the transition from *Pnnm* to $P4_2/mnm$ for $CaBr_2$, which occurs at 553 ºC. [43] Thus, $Ca(BH_4)_2$ and $CaBr_2$ do not have any isostructural relationship in the investigated temperature range, which makes substitution less favorable.

The in situ SR-PXD measurement shows that CaHBr is a decomposition product of the 1:1 $Ca(BH_4)_2$ + $CaBr_2$ mixture above 360 °C. No other crystalline decomposition products are observed.

DSC measured on the 1:1 ratio of $Ca(BH_4)_2$–$CaBr_2$ (not shown) reveal an increase in decomposition temperature which is comparable to that observed for the Cl-substituted sample, even though Br substitution is not taking place. This observation indicate that changed reaction paths, evident from the decomposition products CaHCl and CaHBr, could have a larger impact on the decomposition temperature than the actual halide substitution.

3.5 Theoretical calculations

Theoretical modelling has been used to estimate the solubility of F^-, Cl^- and Br^- into β-$Ca(BH_4)_2$. A single unit cell of β-$Ca(BH_4)_2$ with the *P*-4 symmetry has been considered, and the four BH_4^- units have been progressively substituted by a halide in the case of Cl^- and Br^-, while F substituted H-atoms rather than whole BH_4^- groups. Since the unit cell

of the pure β-$Ca(BH_4)_2$ ($Ca_4B_4H_{16}$) contains 16 H-atoms, a very large number of symmetry-non-equivalent configurations should be considered for single H-to-F substitutions in the BH_4^- units. So, F-substitution has been conducted following the same procedure described for orthorhombic $LiBH_4$,[45] where a "locality principle" was established. It simply states that the lowest energy is obtained when all four H-atoms are substituted by F-atoms in the BH_4^- units. As a consequence, only BF_4^- to BH_4^- unit substitutions have been considered. A single substitution corresponds to a fraction x=0.25, two substitutions to x=0.50 and, finally, three substitution to x=0.75. It has to be noticed that for x=0.5, two possible configurations are possible. In this case, the solution with the lowest energy was considered. The results, expressed in terms of enthalpy of mixing as a function of composition, are reported in Figure 4.

It is clear that BF_4^- substitution leads to a significant positive enthalpy of mixing, suggesting strong immiscibility. On the other hand, both Cl^- and Br^- substitutions appear more favorable, giving an enthalpy of mixing close to zero. As shown in Figure 4, the enthalpy of mixing in the case of x=0.75 gives a negative value around -3 kJ mol^{-1} per formula unit for both Cl^- and Br^- substitutions. The two cases are however very different with respect to variation of the unit cell volume, as shown in Figure 5, where the calculated volume variation of the unit cell is shown as a function of halide substitution. A decrease in volume is indeed computed for Cl^- substitution, in line with the experimental trend. Calculations suggest that a maximum volume change occurs at x=0.75. Calculated values are underestimated, with respect to experimental results, by a few percent points, due to systematic errors of the adopted functionals and basis set or to neglecting temperature effects in the calculations. Calculated volume variations for Br^- substitution are much smaller in comparison to those obtatined for Cl^- substitution, giving an almost constant volume as a function of composition. This behavior can be easily rationalized on the basis of the ionic radius of Br^-, which is much closer to BH_4^- than Cl^-. In turn, the significant volume decrease for the Cl^- substituted structures forces the BH_4 group to rotate in such a way that the H-H intermolecular repulsive contacts are minimized. This effect does not occur for the Br substituted structures, as the volume change is minor compared to pure $Ca(BH_4)_2$ and, consequently, the BH_4 groups maintain their pristine orientation. The computed structural data (not reported here for brevity) shows that the unit cell contraction for x=0.5 Cl^- is anisotropic (see Table S1 in

Supplementary Information) with larger change in *a*- than *c*-axis, in agreement with the experiments (see Table 1).

In order to estimate the solubility of Cl^- and Br^- in β-$Ca(BH_4)_2$ from mixtures with the corresponding halides, thermodynamics of $CaCl_2$ and $CaBr_2$ compounds have to be considered. For both $CaCl_2$ and $CaBr_2$, the most stable structure at T = 25 ^oC has the *Pnnm* symmetry. To estimate the effect of halide substitution, the free energy of $CaCl_2$ and $CaBr_2$ structures have been computed considering, as a reference, the high-temperature structures, crystallizing with the $P4_2/mnm$ symmetry.[43] In order to be coherent, the thermodynamic data have been recalculated considering the two structures within the *P*-4 symmetry (subgroup of $P4_2/mnm$) of the reference β-$Ca(BH_4)_2$ structure, obtaining very similar results (see Tables S1 and S2 in Supplementary Information). The predicted structures of the two high temperature phases are in good agreement with the experimental data, as shown in Table S2 in Supplementary Information. Calculations at T = 25 ^oC on $CaCl_2$ give ΔH = -6.8 kJ mol^{-1} per formula unit and ΔS = 0.5 J mol^{-1} K^{-1} per formula unit, respectively, for the phase transition from the $P4_2/mnm$ to the *Pnnm* structure. Calculations on $CaBr_2$ led to a lower enthalpy change, corresponding to a value of ΔH = -3.0 kJ mol^{-1} per formula unit, but a much higher entropy change, equal to ΔS = -5.3 J mol^{-1} K^{-1} per formula unit. This large variation of entropy for $CaBr_2$ compared to $CaCl_2$ may result from the fact that very low vibrational frequencies, which dominate the entropy value, are much smaller for $CaBr_2$ than for $CaCl_2$, due to the higher mass of Br. The calculated values of enthalpy and entropy should imply a phase transition from orthorhombic (*Pnnm*) to tetragonal ($P4_2/mnm$) symmetry at about 297 ^oC for $CaBr_2$, underestimated with respect to the experimental transition temperature of 553^oC. On the contrary, a higher stability of *Pnnm* with respect to the $P4_2/mnm$ structure is predicted at all temperatures for the $CaCl_2$ crystal.

According to thermodynamic calculations, a similar behavior is expected for Br^- and Cl^- substituted solid solutions. In particular, considering ideal entropy of mixing, a negative free energy of mixing is expected at about 350 °C. In addition, the calculated closer stability of the $P4_2/mnm$ structure with respect to the *Pnnm* for $CaBr_2$ compared to $CaCl_2$ would suggest an easier solubility. The reasons for the disagreement between the calculations and experimental findings are not clear. It could be that kinetic effects,

related to ionic size, play a crucial role during experiments. The discrepancies could also be due to uncertainties in the calculations, as the absence of the predicted *Pnnm* to *P*4$_2$/*mnm* phase transformation for $CaBr_2$ in the experimentally explored temperature range, can hinder the predicted solubility. It is worth noting that a stabilization of β-$Ca((BH_4)_{1-x}Cl_x)_2$ solid solutions with respect to pure β-$Ca(BH_4)_2$ reduces the driving force for the transformation into dehydrogenated products, and thus possibly increasing the dehydrogenation temperature, as observed experimentally (see Figure 3).

The concept of anion substitution in borohydrides remains not fully explored, however, some trends in the structural chemistry are revealed from this work and the literature. For substitution of borohydrides with the heavier halides, (i) the solid containing the smaller anion, e.g. $CaCl_2$, tends to dissolve into the compound containing the larger anion, β-$Ca(BH_4)_2$, and the structure of the latter tends to be preserved in the obtained solid solution. This trend can be interpreted as an increase in the lattice energy due to the clearly observed decrease in the unit cell volume, which may create an internal 'chemical pressure'.[46] (ii) some polymorphs of metal borohydrides are more prone to perform anion substitution, than others, e.g. β-$Ca(BH_4)_2$ and not α-$Ca(BH_4)_2$ as shown here. (iii) This work also high-light that isomorphism may be more important to facilitate anion substitution as compared the similarities in anion radii. This explains that $CaBr_2$ did not dissolve in $Ca(BH_4)_2$, despite the fact that $r(BH_4^-) \sim r(Br^-)$. In fact, in some cases anion substitution may occur in both compounds, which is previously observed for the systems, LiBH4-LiBr, LiBH4-LiI and NaBH4-NaCl systems, possibly due to the fact that β-LiBr, β-LiI and h-$LiBH_4$ as well as NaBH4 and NaCl are isostructural.[47-50]

4. Conclusion

Possible halide substitutions in $Ca(BH_4)_2$ have been investigate by experimental and theoretical (ab-initio) methods. For mixtures with CaX_2, X = F, Cl and Br, substitution is only observed for $CaCl_2$, and no substitution with CaF_2 and $CaBr_2$ was found.

The absence of solid solubility in the $Ca(BH_4)_2$ – CaF_2 system is rationalized by a positive calculated enthalpy of mixing. Substitution with Cl^- is only observed into the β-modification of $Ca(BH_4)_2$ after heating the ball milled sample above 250 °C which is above the orthorhombic-to-tetragonal phase transformation temperature for $CaCl_2$, while

no substitution is observed in α-$Ca(BH_4)_2$. This is explained by the isostructural relationship between β-$Ca(BH_4)_2$ and the tetragonal high-temperature modification of $CaCl_2$. The resulting phase $Ca(BH_4)_{1-x}Cl_x$ has been observed with x from 0 to 0.6, depending on the $Ca(BH_4)_2$:$CaCl_2$ ratio in the initial mixture. However, it is possible that there is full solubility between the two phases due to their isostructural relationship. The decomposition temperature of β-$Ca((BH_4)_{0.5}Cl_{0.5})_2$ was found to be slightly increased compared to pure $Ca(BH_4)_2$, likely due to a reduction of driving force for the dehydrogenation reaction. Br^- substitution in β-$Ca(BH_4)_2$ is predicted by theoretical calculations, but it is not observed experimentally. This is explained by the lack of orthorhombic-to-tetragonal phase transition in the experimental temperature range even though it is predicted by the calculations.

Acknowledgements

This work was financially supported by the European Commission FP7 project FLYHY (grant no. 226943) and the RENERGI and SYNKNØYT programs of the Research Council of Norway. The skilful assistance from the project team at the Swiss-Norwegian Beam Line at the ESRF is gratefully acknowledged.

References

(1) Schlapbach, L.; Zuttel, A. *Nature* **2001**, *414*, 353.

(2) Bogdanovic, B.; Schwickardi, M. *J. Alloys Compd.* **1997**, *253-254*, 1.

(3) Bellosta von Colbe, J. M.; Metz, O.; Lozano, G. A.; Pranza, P. K.; Schmitz, H. W.; Beckmann, F.; Schreyer, A.; Klassen, T. D., M. . *Int. J. Hydrogen Energy* **2012**, *37*, 2807.

(4) Li, H.-W.; Yan, Y.; Orimo S. Züttel, A.; Jensen, C. M. *Energies* **2012**, *4*, 185.

(5) Rude, L. H.; Nielsen, T. K.; Ravnsbaek, D. B.; Bösenmerg, U.; Ley, M. B.; Richter, B.; Arnbjerg, L. M.; Dornheim, M.; Filinchuk, Y.; Besenbacher, F.; Jensen, T. R. *Physica Status Solidi A* **2011**, *208*, 1754.

(6) Miwa, K.; Aoki, M.; Noritake, T.; Ohba, N.; Nakamori, Y.; Towata, S.; Zuttel, A.; Orimo, S. *Phys. Rev. B* **2006**, *74*.

(7) Kim, J.-H.; Jin, S.-A.; Shim, J.-H.; Cho, Y. W. *Scripta Materialia* **2008**, *58*, 481.

(8) Ronnebro, E.; Majzoub, E. H. *J. Phys. Chem. B* **2007**, *111*, 12045.

(9) Kim, Y.; Hwang, S.-J.; Shim, J.-H.; Lee, Y.-S. H., H. N.; Cho, Y. W. *J. Phys. Chem. C* **2012**, *116*, 4330.

(10) Riktor, M. D.; Sørby, M. H.; Chlopek, K.; Fichtner, M.; Buchter, F.; Zuettel, A.; Hauback, B. C. *J. Mater. Chem.* **2007**, *17*, 4939.

(11) Riktor, M. D.; Filinchuk, Y.; Vajeeston, P.; Bardaji, E. G.; Fichtner, M.; Fjellvag, H.; Sørby, M. H.; Hauback, B. C. *J. Mater. Chem.* **2009**, *21*, 7188.

(12) Llamas-Jansa, I.; Friedrichs, O.; Fichtner, M.; Bardaji, E. G.; Züttel, A.; Hauback, B. C. *J. Phys. Chem. C* **2012**, *116*, 13472.

(13) Brinks, H. W.; Fossdal, A.; Hauback, B. C. *J. Phys. Chem. C* **2008**, *112*, 5658.

(14) Maekawa, H.; Matsuo, M.; Takamura, H.; Ando, M.; Noda, Y.; Karahashi, T.; Orimo, S. I. *J. Am. Chem. Soc* **2009**, *131*, 894.

(15) Mosegaard, L.; Moller, B.; Jorgensen, J. E.; Filinchuk, Y.; Cerenius, Y.; Hanson, J. C.; Dimasi, E.; Besenbacher, F.; Jensen, T. R. *J. Phys. Chem. C* **2008**, *112*, 1299.

(16) Arnbjerg, L. M.; Ravnsbaek, D. B.; Filinchuk, Y.; Vang, R. T.; Cerenius, Y.; Besenbacher, F.; Jorgensen, J. E.; Jakobsen, H. J.; Jensen, T. R. *Chem. Mater.* **2009**, *21*, 5772.

(17) Lee, J. Y.; Lee, Y. S.; Suh, J. Y.; Shim, J. H.; Cho, Y. W. *J. Alloys Compd.* **2010**, *506*, 721.

(18) Olsen, J. E.; Sørby, M. H.; Hauback, B. C. *J. Alloys Compd.* **2011**, *509*, L228.

(19) Hino, S.; Fonnelop, J. E.; Corno, M.; Zavorotynska, O.; Damin, A.; Richter, B.; Baricco, M.; Jensen, T. R.; Sørby, M. H.; Hauback, B. C. *J. Phys. Chem. C* **2012**, *116*, 12482.

(20) Rude, L. H.; Filinchuk, Y.; Sørby, M. H.; Hauback, B. C.; Besenbacher, F.; Jensen, T. R. *J. Phys. Chem. C* **2011**, *115*, 7768.

(21) Filinchuk, Y.; Chernyshov, D.; Dmitriev, V. *Z. Krist.* **2008**, *223*, 649.

(22) Filinchuk, Y.; Ronnebro, E.; Chandra, D. *Acta Mater.* **2009**, *57*, 732.

(23) Buchter, F.; Lodziana, Z.; Remhof, A.; Friedrichs, O.; Borgschulte, A.; Mauron, P.; Zuttel, A.; Sheptyakov, D.; Barkhordarian, G.; Bormann, R.; Chlopek, K.; Fichtner, M.; Sørby, M.; Riktor, M.; Hauback, B.; Orimo, S. *J. Phys. Chem. B* **2008**, *112*, 8042.

(24) Aoki, M.; Miwa, K.; Noritake, T.; Ohba, N.; Matsumoto, M.; Li, H. W.; Nakamori, Y.; Towata, S.; Orimo, S. *Applied Physics a-Materials Science & Processing* **2008**, *92*, 601.

(25) Barkhordarian, G.; Jensen, T. R.; Doppiu, S.; Bosenberg, U.; Borgschulte, A.; Gremaud, R.; Cerenius, Y.; Dornheim, M.; Klassen, T.; Bormann, R. *J. Phys. Chem. C* **2008**, *112*, 2743.

(26) Lee, Y. S.; Kim, Y.; Cho, Y. W.; Shapiro, D.; Wolverton, C.; Ozolins, V. *Phys. Rev. B* **2009**, *79*.

(27) Buchter, F.; Lodziana, Z.; Remhof, A.; Friedrichs, O.; Borgschulte, A.; Mauron, P.; Zuttel, A.; Sheptyakov, D.; Palatinus, L.; Chlopek, K.; Fichtner, M.; Barkhordarian, G.; Bormann, R.; Hauback, B. C. *J. Phys. Chem. C* **2009**, *113*, 17223.

(28) Noritake, T.; Aoki, M.; Matsumoto, M.; Miwa, K.; Towata, S.; Li, H. W.; Orimo, S. *J. Alloys Compd.* **2010**, *491*, 57.

(29) Frankcombe, T. J. *J. Phys. Chem. C* **2010**, *114*, 9503.

(30) Majzoub, E. H.; Ronnebro, E. *J. Phys. Chem. C* **2009**, *113*, 3352.

(31) Hammersley, A. P. " FIT2D V12.077. Internal Report ESRF-97-HA02T, 1997. Internal Report ESRF-98-HA01T, 1998.."

(32) Rodríguez-Carvajal, J. *Physica B* **1993**, *192*, 55.

(33) Valenzano, L.; Torres, F. J.; Klaus, D.; Pascale, F.; Zicovich-Wilson, C. M.; Dovesi, R. *Z. Phys. Chemie-Int. J. Res. Phys. Chem. Chem. Phys.* **2006**, *220*, 893.

(34) Dovesi, R.; Ermondi, C.; Ferrero, E.; Pisani, C.; Roetti, C. *Phys. Rev. B* **1984**, *29*, 3591.

(35) Nada, R.; Catlow, C. R. A.; Pisani, C.; Orlando, R. *Model. Simul. Mater. Sci. Eng.* **1993**, *1*, 165.

(36) Apra, E.; Causa, M.; Prencipe, M.; Dovesi, R.; Saunders, V. R. *J. Phys.-Condes. Matter* **1993**, *5*, 2969.

(37) Curtiss, L. A.; McGrath, M. P.; Blaudeau, J. P.; Davis, N. E.; Binning, R. C.; Radom, L. *J. Chem. Phys.* **1995**, *103*, 6104.

(38) Grimme, S. *J. Comput. Chem.* **2006**, *27*, 1787.

(39) Pascale, F.; Zicovich-Wilson, C. M.; Gejo, F. L.; Civalleri, B.; Orlando, R.; Dovesi, R. *J. Comput. Chem.* **2004**, *25*, 888.

(40) Tomaszewski, P. E. *Phase Transitions* **1992**, *38*, 127.

(41) Olejak-Chodan, M.; Eick, H. A. *J. Solid State Chem.* **1987**, *69*, 274.

(42) Riktor, M., personal communication.

(43) Howard, C. J.; Kennedy, B. J.; Curfs, C. *Phys. Rev. B* **2005**, *72*.

(44) Vegard, L. *Zeitschrift Fur Physik* **1921**, *5*, 17.

(45) Corno, M.; Pinatel, E.; Ugliengo, P.; Baricco, M. *J. Alloys Comp.* **2011**, *509*, S679.

(46) D'Anna, V.; Daku, L. M. L.; Hagemann, H.; Kubel, F. *Phys. Rev. B* **2010**, *82*, 11.

(47) Olsen, J. E.; Sorby, M. H.; Hauback, B. C. *J. Alloys Compd.* **2011**, *509*, L228.

(48) Rude, L. H.; Zavorotynska, O.; Arnbjerg, L. M.; Ravnsbaek, D. B.; Malmkjaer, R. A.; Grove, H.; Hauback, B. C.; Baricco, M.; Filinchuk, Y.; Besenbacher, F.; Jensen, T. R. *Int. J. Hydrogen Energy* **2011**, *36*, 15664.

(49) Rude, L. H.; Groppo, E.; Arnbjerg, L. M.; Ravnsbaek, D. B.; Malmkjaer, R. A.; Filinchuk, Y.; Baricco, M.; Besenbacher, F.; Jensen, T. R. *J. Alloys Compd.* **2011**, *509*, 8299.

(50) Ravnsbaek, D. B.; Rude, L. H.; Jensen, T. R. *J. Solid State Chem.* **2011**, *184*, 1858.

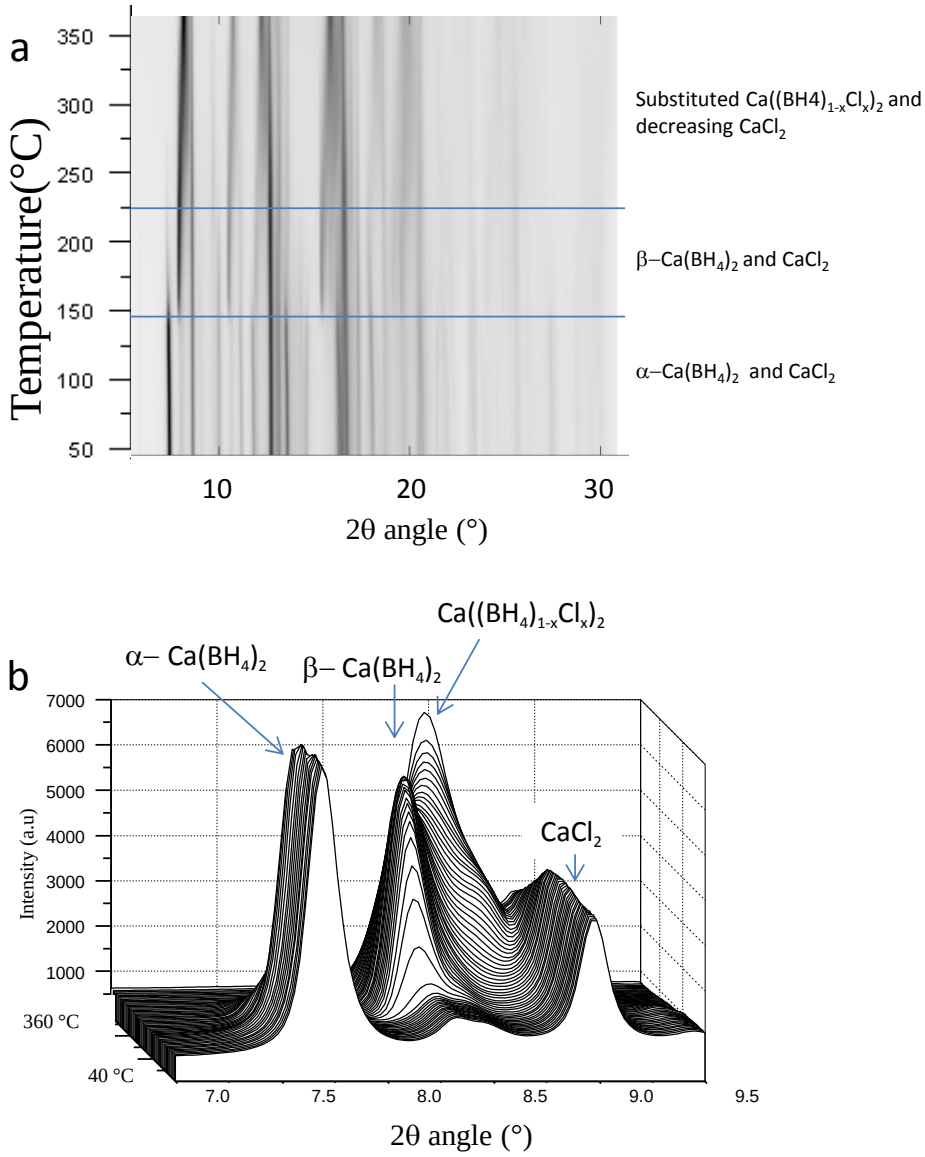

Figure 1 In situ SR-PXD measured for $Ca(BH_4)_2$ + $CaCl_2$ in molar ratio 1:1, heating rate 3 K/min. The temperature increases from 40 to 360 °C. (a) gives a plot of the evolution of intensities at 2θ area. (b) 3D plot of selected 2θ area. λ = 0.703511 Å

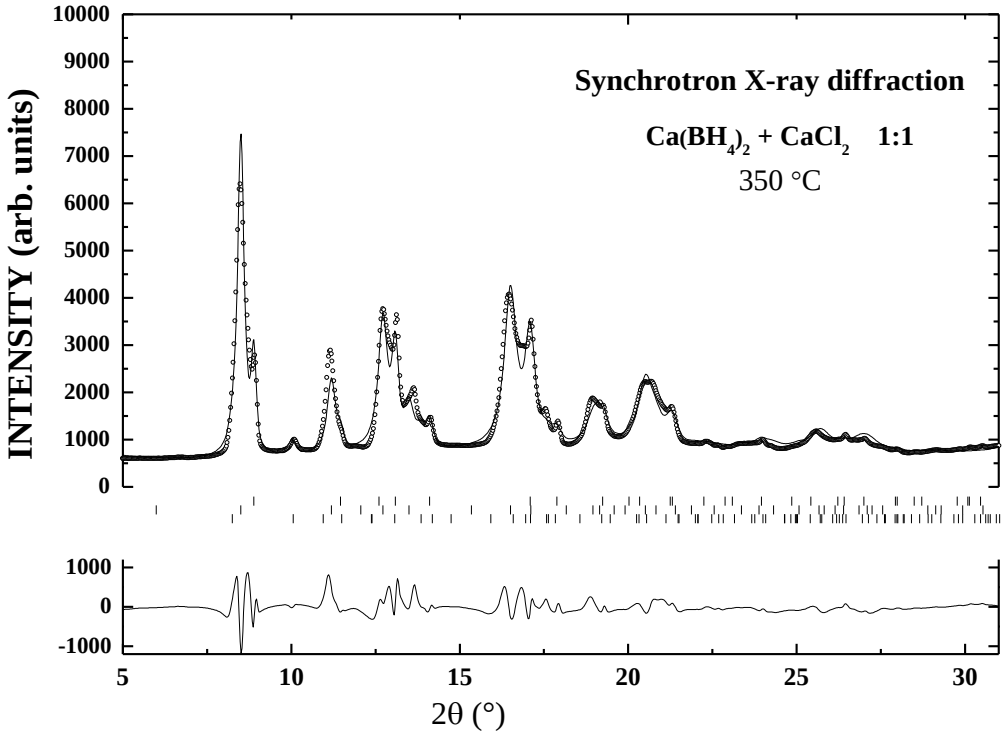

Figure 2. Rietveld refinement for SR-PXD data of ball milled $Ca(BH_4)_2$ and $CaCl_2$ in molar ratio 1:1 at 350 °C. Three phases are refined $CaCl_2$ $P4_2/mnm$ (top), substituted β-$Ca((BH_4)_{1-x}Cl_x)_2$ with x = 0.5 (middle) and $CaCl_2$ *Pbcn* (bottom). Experimental data are shown as dots, and the calculated profile is a solid line. The bottom line shows the difference plot. λ = 0.703511 Å.

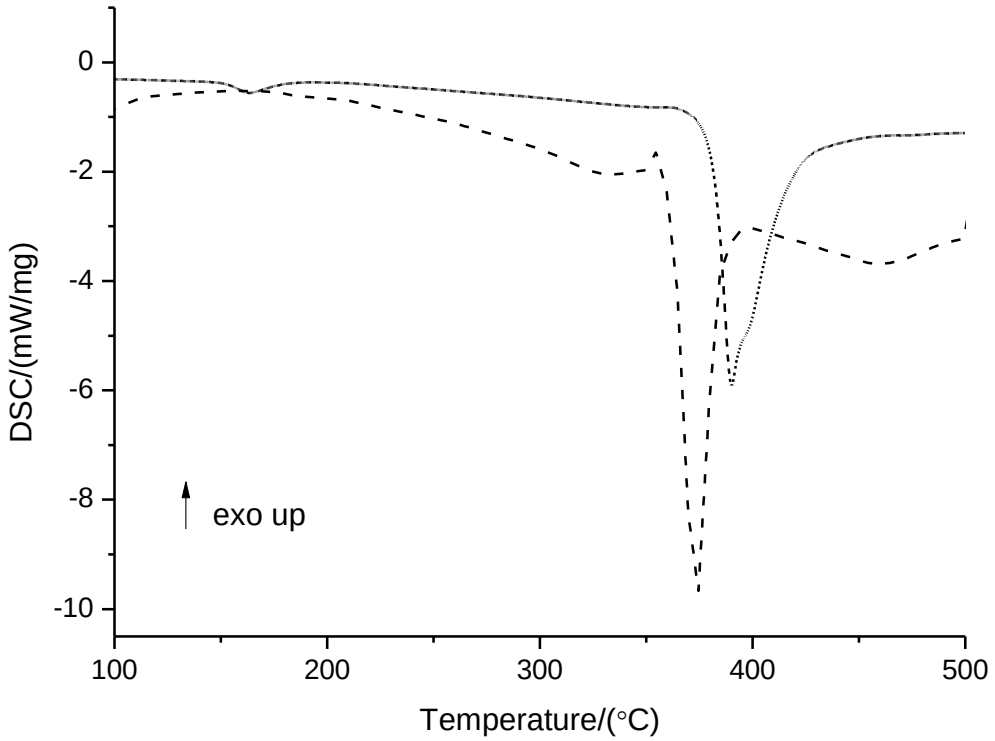

Figure 3. DSC data for $Ca(BH_4)_2$ (dashed) and $Ca(BH_4)_2$–$CaCl_2$ (1:1) (solid) with heating rate 10K/min.

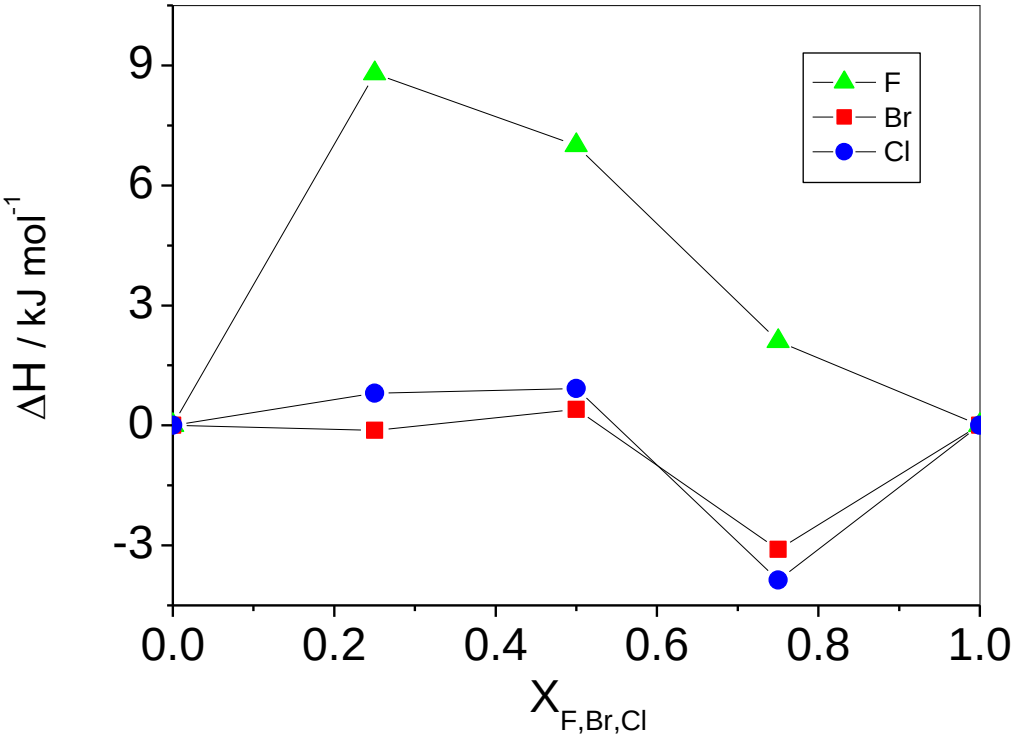

Figure 4. Computed enthalpy of mixing for solid solution of beta calcium borohydride, where BH_4^- units have been progressively substituted by BF_4^-, Cl^- and Br^-. All values are per formula unit.

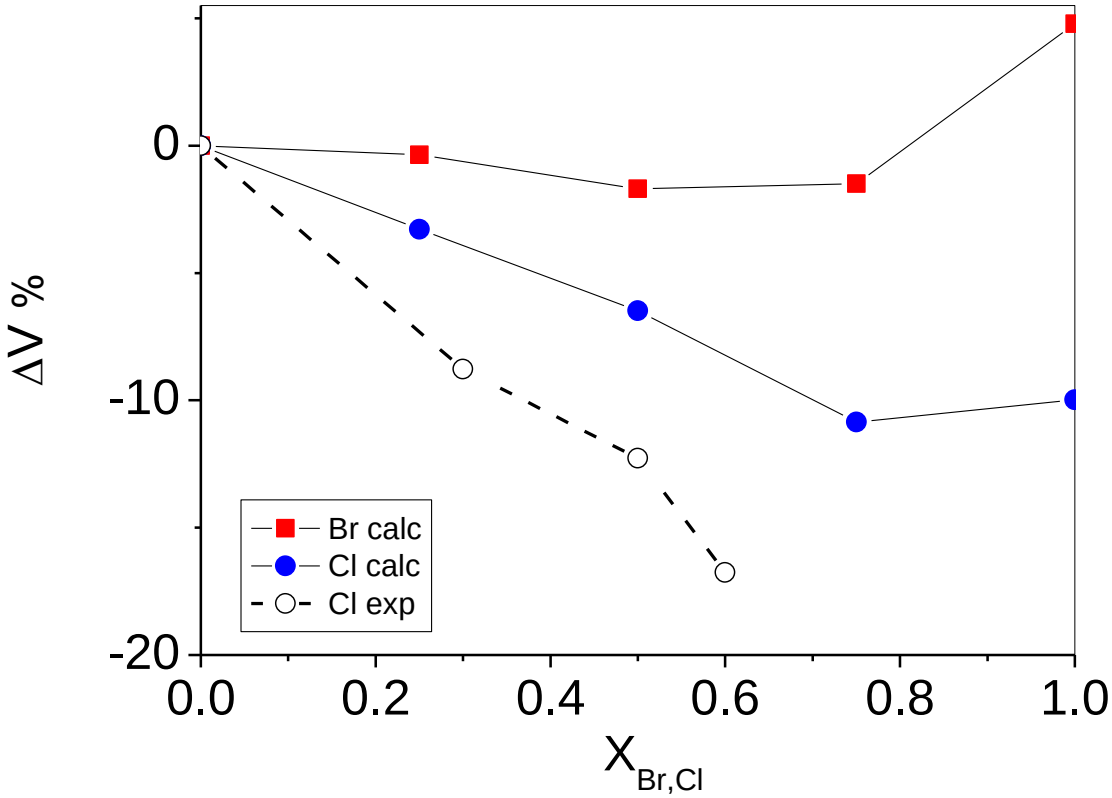

Figure 5. Variations of the unit cell volume for solid solution of β-$Ca(BH_4)_2$, where BH_4^- units have been progressively substituted by Cl^- (circles) and Br^- (squares). Continuous lines (computed), dashed line (experimental).